

Degenerate three-band Hubbard model with anti-Hund's rule interactions: A model for A_xC_{60}

Mats Granath*

NORDITA, Blegdamsvej 17, DK-2100 Copenhagen, Denmark

Stellan Östlund†

Chalmers Technical University, Gothenburg 41296, Sweden

(Received 4 August 2003; published 21 November 2003)

We consider the orbitally degenerate three-band Hubbard model with on-site interactions which favor low spin and low orbital angular momentum using standard second-order perturbation theory in the large Hubbard- U limit. At even-integer filling this model is a Mott insulator with a nondegenerate ground state that allows for a simple description of particle-hole excitations as well as gapped spin and orbital modes. We find that the Mott gap is generally indirect and that the single-particle spectrum at low doping reappears close to even filling but rescaled by a factor of $2/3$ or $1/3$. The model captures the basic phenomenology of the Mott insulating and metallic fullerides A_xC_{60} . This includes the existence of a smaller spin gap and larger charge gap at even-integer filling, the fact that odd-integer stoichiometries are generally metallic while even integer are insulating, as well as the rapid suppression of the density of states and superconducting transition temperatures with doping away from $x=3$.

DOI: 10.1103/PhysRevB.68.205107

PACS number(s): 71.27.+a, 74.70.Wz, 75.10.-b

I. INTRODUCTION

The physics of Mott insulators has emerged as a key ingredient in the study of strongly correlated systems,¹ largely motivated by the understanding that much of the exotic physics of the underdoped cuprate superconductors has connections to the undoped Mott insulating state. The basic model for a Mott insulator discussed in connection with the cuprates is the large- U half-filled Hubbard model. For this model the low-energy spectrum at half filling is reasonably well understood, but the higher-energy spectrum as well as the physics away from half filling is still very much an open problem. Much of the difficulty seems to trace back to the fact that the Mott insulating ground state for this system is not known.

Here we will study a model of a Mott insulator which has a simple nondegenerate ground state and where we can describe the spectrum of excited states and explore the physics at and near the Mott transition in a well controlled manner. The model is a degenerate three channel Hubbard model which has multiplet splitting on-site interactions that favor low spin and low orbital angular momentum. This model is the simplest model with spin and orbital symmetries which at even-integer filling allows for a Mott insulating nondegenerate ground state.² Since the ground state is nonmagnetic, the spin physics which complicates the single-band Hubbard model is absent at low energies. Although interesting in itself as a natural and simplifying extension of the Hubbard model, our main motivation for studying this model is that it very naturally captures some of the most distinctive phenomenology of the alkali doped C_{60} compounds, the fullerides.

Crystalline C_{60} is a band insulator with a completely filled molecular orbital.³ Doping with alkali atoms, forming A_nC_{60} , transfers electrons into the lowest unoccupied molecular orbital (LUMO), which according to elementary molecular theory is threefold degenerate. These form three spin degenerate bands according to the band theory of the crystal.

It is believed that the charge transfer is complete and that the influence of the alkali ions is in general, negligible apart from changing the crystal structure and the corresponding band theory.

If these were simple metals, band theory would predict a metallic state for any doping $0 < n < 6$ and possibly superconductivity with transition temperatures which would follow roughly the density of states at the Fermi energy as the doping is varied. Experimentally, however, it turns out that the compounds with even-integer doping ($n=2,4$) are nonmagnetic insulators⁴⁻⁶ and superconductivity is only seen in a narrow range around half filling ($n=3$) and with transition temperatures that are sharply maximized here.⁷ Band theory augmented by BCS theory of superconductivity fails to reproduce this behavior.

It is well known that correlation effects are important as these are weakly bound molecular solids with a narrow bandwidth of ≈ 0.5 eV and it is believed that the on-site Coulomb repulsion is ≈ 1 eV. One might therefore expect that the system would be a Mott insulator at any integer filling. This, however, does not explain why systems with even-integer filling are generally insulating, while systems with odd-integer filling are generally metallic. A second related question is why the insulating materials at even-integer filling are nonmagnetic. From Hund's rule, we would expect the highest spin configuration to be the molecular ground state, $S=1$ for $n=2$ and $n=4$, and consequently some sort of magnetic ground state is to be expected for the solid.

One explanation for the violation of Hund's rule in the insulating materials is that the Jahn-Teller (JT) effect counteracts Hund's rule, with the lowest-energy JT distorted state of the C_{60} molecule at even-integer occupation being a spin singlet.⁸ However, a problem with the naive Jahn-Teller scenario is that static distortions of the C_{60} molecules have not been detected in solid C_{60} .⁹ Indirect evidence has come from the existence of two energy-gap scales in the insulating systems, a smaller spin gap of around 50 meV and a larger

charge gap of around 500 meV. The larger charge gap is quite clearly a Mott gap related to the intramolecular electron-electron repulsion, whereas the smaller spin gap has been linked to a singlet to triplet gap of JT distorted molecules.⁵

A different scenario for the violation of Hund's rule suggested by Chakravarty *et al.*¹⁰ and Baskaran and Tosatti¹¹ claims that electronic correlations on a C_{60} molecule can break the degeneracy of any partially filled molecular orbital in such a way as to minimize the spin and orbital angular momentum. Chakravarty and co-workers looked at a Hubbard model on single C_{60} molecule, with strong electron-electron repulsion (U) on each carbon atom, using second-order perturbation theory in U . The linear in U terms give Hund's rule with a preferred highest spin configuration which minimizes the overlap between electrons. The second-order term on the other hand prefers low spin configurations with large overlaps which can take better advantage of virtual excitations of the core electrons.¹² The validity of the qualitative features of the perturbation theory is supported by exact diagonalization of smaller Hubbard clusters.¹³

One important feature of the scenario based on intramolecular electronic correlations is that in contrast to the static Jahn-Teller distortions the orbital symmetry of the molecule is preserved. More recently, it has also been emphasized in a series of papers by Tosatti and co-workers¹⁴⁻¹⁷ that Jahn-Teller phonons treated in the antiadiabatic limit will also give rise to an effective electronic Hamiltonian with inverse Hund's rule which preserves the orbital symmetry of the molecule. It may thus be difficult to distinguish the latter scenario from the one based on electronic correlations and a full treatment of both the electron-electron and the electron-lattice interactions to decide which energy scales dominate is asked for. Along these lines a recent density-functional calculation does find that Hund's rule is valid for an isolated C_{60} and only counteracted by the JT effect,¹⁸ although issues such as electronic screening by the surrounding molecules may also be important.¹⁹

Regardless of the mechanism behind the inversion of Hund's rule on the C_{60} molecule it is an interesting problem to study the effective model of solid C_{60} which this naturally gives rise to, namely the three channel Hubbard model with "anti-Hund's rule" interactions. Here we study this model in the limit of strong interactions where we can do standard second-order perturbation theory in the intermolecular hopping. We find that the even/odd integer doping effect, the existence of two energy gaps in the insulating systems, as well as the rapid variation of T_c with doping away from $n = 3$ are all natural consequences of this model.

We will focus primarily on even integer filling ($n = 2$ or 4), where the problem simplifies significantly because of the resultant nondegenerate strong-coupling ground state. Based on this we can describe the spectrum consisting, in general, of an indirect Mott gap to particle-hole excitations and chargeless spin and orbital modes with a distinct energy gaps. We also derive the spectrum of a single particle or hole doped into the nonmagnetic Mott insulator. The particle and hole spectra turns out to be exactly the same as the noninteracting band structure up to an overall rescaling of the hop-

ping by a factor of 1/3 or 2/3. These characteristic properties of the nonmagnetic Mott insulator are in agreement with previous results on the same model.^{14,15}

Apart from the correspondence with the physics of the Mott insulating A_2C_{60} and A_4C_{60} our main conclusion is that C_{60} with a filling $n = 2 + x$ or $4 + x$ of the LUMO band, with $|x| \ll 1$, is best understood as a *doped Mott insulator*, manifested by a charge-carrier concentration given by $|x|$ instead of n . In addition, the density of states is up to a rescaling factor, the same as that of the noninteracting band structure at the band edges $n = |x|$ or $n = 6 - |x|$ for particle and hole doping, respectively. If we heuristically extend these results to larger $x \approx 1$, the observed *variation of T_c* with doping, for $2 < n < 4$, follows naturally within any weak-coupling BCS-like scenario as a consequence of the rapid drop in the density of states close to noninteracting band edges.

We will not, however, discuss the actual mechanism of superconductivity, i.e., the source of pairing. In particular, we will not assume that the intramolecular singlet-triplet gap is necessarily large enough to overcome the Coulomb repulsion and give rise to a bare attraction along the lines of the earlier work.^{10,11} In fact, a fit of the parameters of the model to experiment suggests that this is not the case. Nevertheless, any other mechanism, such as one based on attraction from electron-phonon interactions, certainly needs to include the strong electron correlations which are present as indicated most clearly by existence of Mott insulating phases.

The paper is organized as follows. In Sec. II we define the model and the strong-coupling limit we will primarily consider. Then we derive a perturbative effective Hamiltonian valid in the strong-coupling limit. In Sec. III we study the Mott insulator at even integer filling and describe the spectrum of excited states. We also discuss the distinction between even and odd-integer dopings and why at odd-integer doping the system is more likely to be on the metallic side of the Mott transition. Then we use the results derived for the model to get an estimate of the parameters by comparing to experiment on A_2C_{60} and A_4C_{60} . In Sec. IV we study the doped Mott insulator at a filling close to even integer and speculate on the implications of these results to the whole doping range $2 < n < 4$ as well as the properties at higher temperatures. Finally, in Sec. V we conclude.

II. THE MODEL

We will be studying a three-band Hubbard model. The electrons occupy three degenerate p orbitals ($L = 1$) on every site of the lattice and we define electron creation and destruction operators $c_{r,ls}^\dagger$ and $c_{r,ls}$ with site index, orbital quantum number and spin, respectively. We will be working in the L^2 basis where $l = -1, 0, 1$.

The Hamiltonian reads

$$H = h + H_I \quad (1)$$

with a nearest-neighbor hopping

$$h = \sum_{\langle rr' \rangle} t_{ll'}^{rr'} c_{r,ls}^\dagger c_{r',l's} \quad (2)$$

and on-site interaction

$$H_I = \sum_r \frac{1}{2} U n_r^2 + J_L \vec{L}_r^2 + J_S \vec{S}_r^2, \quad (3)$$

with $U, J_L, J_S > 0$. Here

$$n_r = \sum_{l,s} c_{r,ls}^\dagger c_{r,ls}, \quad (4)$$

$$\vec{L}_r = \sum_{ll's} c_{r,ls}^\dagger \vec{L}_{l,l'} c_{r,l's}, \quad (5)$$

$$\vec{S}_r = \sum_{lss'} c_{r,ls}^\dagger \vec{S}_{s,s'} c_{r,l's'} \quad (6)$$

are the number, orbital angular momentum, and spin operators, respectively.

The lattice is three dimensional and we assume a point-group symmetry which is such that the hopping preserves the threefold orbital degeneracy, although this may be relaxed as long as the symmetry breaking crystal field is small compared to the interactions. We are going to study this in the strong coupling limit defined as

$$U \gg J_S \gg J_L \gg t, \quad (7)$$

where $t = \max(t_{ll'}^{rr'})$. For C_{60} band-structure calculations²⁰ give $t \sim 100$ meV and values of U of the order of 1 eV have been suggested.³ A subsequent fit of the parameters of the model to experiment on $A_n C_{60}$ suggests that the large- U limit is quite well satisfied with $U/t \approx 5$, while $J_S \sim J_L \sim t$. The limit $U \gg t$ is essential for our treatment, while relaxing the other limits probably will not change the qualitative features of our results.

At $t=0$ we find that the Hamiltonian is simply diagonalized in terms of the states $|n, L, S, L^z, S^z\rangle_r$ with n the number of electrons on a site and (L, S) the total angular momentum and spin and the energy $E(n, L, S) = \frac{1}{2} U n^2 + J_L L(L+1) + J_S S(S+1)$. In the strong-coupling limit the effect of the hopping t will be to reduce the translational degeneracy. It is the topic of the following section to derive an effective Hamiltonian which describes these low energy degrees of freedom.

A. Effective strong-coupling Hamiltonian

Let us define the short-hand notation $p = (n, L, S)$ and $\alpha = (L^z, S^z)$. As shown in Table I any single-site states $|p, \alpha\rangle_r$ and $|p', \alpha'\rangle_{r'}$ have the same energy, barring accidental degeneracies, if and only if $p = p'$. This implies that any eigenstate of H_I will not mix different representations at a site and can be written as $\Pi_r \psi_{p,\alpha}^r |p, \alpha\rangle_r$, where $\psi_{p,\alpha}^r \neq 0$ only for one particular $p(r)$. Consider now the action of the hopping term h on an eigenstate. This will affect two arbitrary nearest-neighbor sites r and r' , giving $|p, \alpha\rangle_r |p', \alpha'\rangle_{r'} \xrightarrow{t} \sum_{q\beta q'\beta'} M |q, \beta\rangle_r |q', \beta'\rangle_{r'}$, where M are the matrix elements of h between the in and out states. Unless the initial and final nearest-neighbor states have only exchanged par-

TABLE I. Spectrum of the interaction, Eq. (3), at a single site with states specified by occupation n , total orbital angular momentum L and total spin S .

n	(L, S)	E
0	(0,0)	0
1	$(1, \frac{1}{2})$	$\frac{1}{2}U + 2J_L + \frac{3}{4}J_S$
2	(0,0), (2,0), (1,1)	$2U + \{0, 6J_L, 2J_L + 2J_S\}$
3	$(1, \frac{1}{2}), (2, \frac{1}{2}), (0, \frac{3}{2})$	$\frac{9}{2}U + \{2J_L + \frac{3}{4}J_S, 6J_L + \frac{3}{4}J_S, \frac{15}{4}J_S\}$
4	(0,0), (2,0), (1,1)	$8U + \{0, 6J_L, 2J_L + 2J_S\}$
5	$(1, \frac{1}{2})$	$\frac{25}{2}U + \frac{3}{4}J_S$
6	(0,0)	18U

title number and representation between the sites, i.e., $q = p'$ and $q' = p$, there will be a nonzero energy difference $\Delta E = E(q) + E(q') - E(p) - E(p')$ with respect to H_I , which is some linear combination of U, J_L, J_S . In the strong-coupling limit Eq. (7) there is no accidental degeneracy and the energy difference satisfies $\Delta E \gg t$, which will allow us to do a perturbation theory in $t/\Delta E$. Henceforth we will use the ΔE , to define the absolute value of the minimum nonzero energy difference between two different nearest neighbor state configurations. From Table I we can check that in the strong-coupling limit this corresponds to $\Delta E = 4J_L$, given for instance by $E(3, 2, \frac{1}{2}) + E(2, 0, 0) - E(2, 0, 0) - E(3, 1, \frac{1}{2})$.

We will be using the effective Hamiltonian method described as applied to the one-band Hubbard model in, for instance, Fazekas.²¹ We introduce a canonical transformation

$$\mathcal{H}_{eff} = e^{iS} \mathcal{H} e^{-iS} = \mathcal{H} + i[S, \mathcal{H}] + \frac{i^2}{2} [S, [S, \mathcal{H}]] + \dots, \quad (8)$$

where the goal is to find \mathcal{H}_{eff} such that it does not couple the different energy sectors of H_I .

Let us consider h as a matrix which acts on nearest-neighbor states $|p, \alpha\rangle_r |p', \alpha'\rangle_{r'} = |a\rangle_{rr'}$ which in a short-hand notation we will denote by a single index a, b, c, \dots . We write

$$h = \sum_{\langle rr' \rangle} h^{rr'} = \sum_{\langle rr' \rangle} h_{ab}^{rr'} |a\rangle_{rr'} \langle b|_{rr'}, \quad (9)$$

where

$$h_{ab}^{rr'} = \langle a|_{rr'} \sum_{ll'} t_{ll'}^{rr'} (c_{r,ls}^\dagger c_{r',l's} + \text{H.c.}) |b\rangle_{rr'}. \quad (10)$$

Next we split $h_{ab}^{rr'}$ into $h_{ab}^{rr'} = h_{ab}^{0,rr'} + h_{ab}^{1,rr'}$, where $h_{ab}^{0,rr'} = h_{ab}^{rr'} \delta_{E(a), E(b)}$ only connects states with the same energy and $h_{ab}^{1,rr'} = h_{ab}^{rr'} - h_{ab}^{0,rr'}$ which connects states with different energy. It follows that we can also write $h = h^0 + h^1$.

We introduce $\mathcal{S} = \mathcal{S}_1 + \mathcal{S}_2$, where $\mathcal{S}_1 \sim \mathcal{O}(t/\Delta E)$ and $\mathcal{S}_2 \sim \mathcal{O}(t^2/\Delta E^2)$ and expand Eq. (8) to $\mathcal{O}(t^2/\Delta E)$,

$$\begin{aligned} \mathcal{H}_{eff} = & H_I + h^0 + h^1 + i[\mathcal{S}_1, H_I] + i[\mathcal{S}_1, h^0 + h^1] \\ & + \frac{i^2}{2}[\mathcal{S}_1, [\mathcal{S}_1, H_I]] + i[\mathcal{S}_2, H_I]. \end{aligned} \quad (11)$$

To first order in t we want to cancel h^1 by taking \mathcal{S}_1 to solve

$$i[\mathcal{S}_1, H_I] = -h^1. \quad (12)$$

Clearly \mathcal{S}_1 needs to act only on nearest-neighbor sites. Defining $\mathcal{S}_1 = \sum_{\langle rr' \rangle} \mathcal{S}_1^{rr'} = \sum_{\langle rr' \rangle} \mathcal{S}_{1,ab}^{rr'} |a\rangle_{rr'} \langle b|_{rr'}$ gives from Eq. (12)

$$\begin{aligned} i \sum_{\langle rr' \rangle} h^{1,rr'} \\ = \sum_{\langle rr' \rangle r''} [\mathcal{S}_1^{rr'}, H_I^{r''}] &= \sum_{\langle rr' \rangle} \mathcal{S}_{1,ab}^{rr'} [|a\rangle_{rr'} \langle b|_{rr'}, H_I^r + H_I^{r'}] \\ = \sum_{\langle rr' \rangle} \mathcal{S}_{1,ab}^{rr'} (E(b) - E(a)) & |a\rangle_{rr'} \langle b|_{rr'}, \end{aligned} \quad (13)$$

where we have used the fact that we work in the eigenbasis of H_I such that $(H_I^r + H_I^{r'}) |a\rangle_{rr'} = E(a) |a\rangle_{rr'}$. We thus arrive at the solution

$$\mathcal{S}_{1,ab}^{rr'} = \frac{ih_{ab}^{1,rr'}}{E(b) - E(a)}. \quad (14)$$

Recall that $h_{ab}^{1,rr'}$ is defined as only having nonzero entries when $|E(b) - E(a)| \geq \Delta E$ so that $\mathcal{S}_1 \sim t/\Delta E$.

Given the solution for \mathcal{S}_1 obeying Eq. (12) we can rewrite Eq. (11) as

$$\begin{aligned} \mathcal{H}_{eff} = & H_I + h^0 + i[\mathcal{S}_1, h^0 + h^1] - \frac{i}{2}[\mathcal{S}_1, h^1] + i[\mathcal{S}_2, H_I] \\ = & H_I + h^0 + i[\mathcal{S}_1, h^0] + \frac{i}{2}[\mathcal{S}_1, h^1] + i[\mathcal{S}_2, H_I]. \end{aligned} \quad (15)$$

In analogy to using \mathcal{S}_1 to cancel terms linear in t which connect different energy subsectors we can now use \mathcal{S}_2 to cancel similar terms to order t^2 which arise from the commutators of \mathcal{S}_1 and h in Eq. (15). Technically this is slightly more involved because there is also three site next-nearest-neighbor interactions generated to second order in t and we refer the reader to the Appendix for the details.

The final expression for the effective strong-coupling Hamiltonian reads

$$\begin{aligned} \mathcal{H}_{eff} = & H_I + \sum_{\langle r, r', r'' \rangle, ab} (\mathcal{H}_{eff}^{rr'})^{rr'} |a\rangle_{rr'} \langle b|_{rr'} \\ & + \sum_{\langle r, r', r'' \rangle, ab} (\mathcal{H}_{eff}^{rr' r''})^{rr' r''} |a\rangle_{rr' r''} \langle b|_{rr' r''} + \mathcal{O}(t^3/\Delta E^2), \end{aligned} \quad (16)$$

with

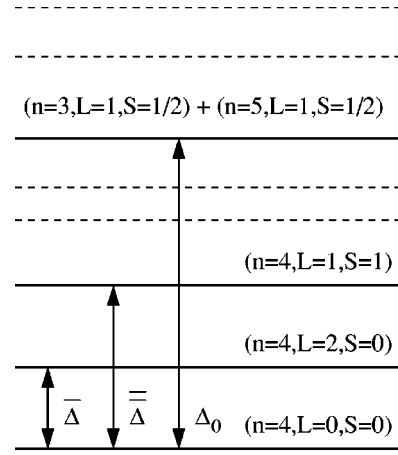


FIG. 1. Spectrum at $t=0$ and doping $n=4$ showing the lowest-energy excitations of the three distinct kinds discussed in the text.

$$(\mathcal{H}_{eff})_{ab}^{rr'} = \left(h_{ab}^{rr'} - \sum_{c, E(c) \neq E(a)} \frac{h_{ac}^{rr'} h_{cb}^{rr'}}{E(c) - E(a)} \right) \delta_{E(a), E(b)}, \quad (17)$$

$$(\mathcal{H}_{eff})_{ab}^{rr' r''} = -\frac{1}{2} \sum_{c, E(c) \neq E(a)} \frac{h_{ac}^{rr'} h_{cb}^{r' r''} + h_{ac}^{r' r''} h_{cb}^{rr'}}{E(c) - E(a)} \delta_{E(a), E(b)}. \quad (18)$$

Here $|a\rangle_{rr'} = |n, L, S, L^z, S^z\rangle_r |n', L', S', L'^z, S'^z\rangle_{r'}$ and $|a\rangle_{rr' r''}$ are arbitrary nearest-neighbor and next-nearest-neighbor eigenstates of H_I with energy $E(a)$ and $h_{ab}^{rr'}$ is defined according to Eq. (10) with a straightforward extension for three-site states.

III. THE MOTT INSULATOR

In the strong-coupling limit, Eq. (7), of this model the system is an insulator at any integer filling with a gap to charge-carrying excitations of the order of U . At odd integer filling the ground state is the highly degenerate $|GS, 1/3/5\rangle = |\Pi_r, n=1/3/5, L=1, S=1/2, L^z, S^z\rangle_r$ and the hopping t will introduce strong correlations in analogy with the half-filled single-band Hubbard model. We will return to this problem briefly in discussing the fact that A_3C_{60} is generally on the metallic side of the Mott transition.

However, at even integer filling, $n=2$ or 4 , the ground state is nondegenerate, $|GS, 2/4\rangle = |\Pi_r, n=2/4, L=0, S=0\rangle_r$. Here, we will find that much of the physics can be understood in terms of a simple noninteracting single-particle picture. This will be the focus of the subsequent discussion and the main issue of the paper. We will discuss $n=4$ to compare with experiments on K_4C_{60} and Rb_4C_{60} but the treatment of $n=2$ is completely analogous.

At filling $n=4$ there are three types of excitations of the ground state that can be readily identified and which are indicated in Fig. 1. We can excite a single site into a higher-energy multiplet, creating states $|4, 2, 0, L^z\rangle_r, |\Pi_{r' \neq r}, 4, 0, 0\rangle_{r'}$ or $|4, 1, 1, L^z, S^z\rangle_r, |\Pi_{r' \neq r}, 4, 0, 0\rangle_{r'}$ with energy $\bar{\Delta} \equiv E(4, 2, 0) - E(4, 0, 0) = 6J_L$ and $\bar{\Delta} \equiv E(4, 1, 1) - E(4, 0, 0) = 2J_L + 2J_S$,

respectively. There is also “particle-hole” excitations in different multiplets, the one with lowest energy being $|3,1,\frac{1}{2},L^z,S^z\rangle_r|5,1,\frac{1}{2},L'^z,S'^z\rangle_{r'}\Pi_{r''\neq r,r'}|4,0,0\rangle_{r''}$ with energy $\Delta_0=U+4J_L+\frac{3}{2}J_S$. The energy Δ_0 is the Mott gap to zeroth order in t .

The degeneracy of the excited states will be lifted by the hopping h and using the effective Hamiltonian Eq. (17) we can study the spectrum perturbatively in t .

A. Spin gap, spin and orbital modes

The spin and orbital excitations $|4,1,1,L^z,S^z\rangle_r\Pi_{r'\neq r}|4,0,0\rangle_{r'}$ and $|4,2,0,L^z\rangle_r\Pi_{r'\neq r}|4,0,0\rangle_{r'}$ are degenerate in L^z and S^z as well as position r . Acting with the effective Hamiltonian Eq. (17) will split the degeneracy in space (as well as the orbital degeneracy) leading to a band description of these states. Clearly to first order in h (t), the effective Hamiltonian will not affect these states as it necessarily creates a high-energy particle-hole state. For the same reason the second-order three-site interaction will not contribute. However, the second-order nearest-neighbor term can hop the excited state at r to a nearest neighbor r' or to the same site r through an intermediate particle-hole state.

Focusing on the spinless excitations we define the “bosonic” operator

$$b_{r,m}^\dagger = |4,2,0,m\rangle_r \langle 4,0,0|_r \quad (19)$$

in terms of which we can write an excited orbital state as $b_{r,m}^\dagger|GS,4\rangle$. These operators do not obey proper commutation relations but if we consider only single-particle physics this is irrelevant. With these operators we can write the following single-particle Hamiltonian describing the dynamics of such excitations:

$$H = \sum_{\langle r,r'\rangle} \bar{t}_{mm'}^{rr'} b_{r,m}^\dagger b_{r',m'} + \sum_r \bar{t}_{mm'} b_{r,m}^\dagger b_{r,m}, \quad (20)$$

where

$$\begin{aligned} \bar{t}_{mm'}^{rr'} &= -\frac{1}{U+3/2J_S-2J_L} \\ &\times \sum \langle 4,2,0,m|_r \langle 4,0,0|_{r'} t_{ii'}^{rr'} (c_{r,is}^\dagger c_{r',i's} + \text{H.c.}) | \text{ph} \rangle \\ &\times \langle \text{ph} | t_{jj'}^{rr'} (c_{r,js}^\dagger c_{r',j's} + \text{H.c.}) | 4,0,0 \rangle_r | 4,2,0,m' \rangle_{r'}, \end{aligned} \quad (21)$$

and similarly for $\bar{t}_{mm'}$. Here $|\text{ph}\rangle$ are particle-hole states $|5,1,\frac{1}{2},l,s\rangle_r|3,1,\frac{1}{2},l',s'\rangle_{r'}$ (or with reversed positions) and the sum is over all indices except m,m' and r,r' . Similar contributions but with larger denominators from intermediate particle-hole excitations in higher-energy multiplets have been ignored in Eq. (21).

Deriving the Hamiltonian Eq. (20) is thus a straightforward problem. The Hamiltonian is noninteracting and can in principle be diagonalized in momentum space. In general the five orbital components will be mixed with a complicated band structure. The same calculation can be carried out for

the spinful ($n=4,L=1,S=1$) states, where there are nine coupled states per site. Although the bandwidth of these spin and orbital modes are naively of the order of t^2/U the high degeneracy of these states is expected to give a significant broadening of bandwidth, perhaps by a factor of the spin and orbital degeneracies of these states. The spinful excitations should be readily detectable experimentally as a band of magnons with some gap Δ_s , a spin gap. We will return to the issue of the spin modes in discussing NMR on A_2C_{60} and A_4C_{60} .

B. Charge excitations

At filling $n=4$ the lowest-energy charge-carrying excitations are the particle-hole states $|3,1,\frac{1}{2},l,s\rangle_r|5,1,\frac{1}{2},l',s'\rangle_{r'}\Pi_{r''\neq r,r'}|4,0,0\rangle_{r''}$ with an energy $\Delta_0=U+4J_L+\frac{3}{2}J_S$. Acting with the effective Hamiltonian Eq. (17) on such a state will translate either the particle ($n=5$) or the hole ($n=3$) to a nearest-neighbor site through the linear term in h (t). To second order, there is next-nearest-neighbor hopping through an intermediate state in a higher-energy multiplet. Since it is higher-order, $\mathcal{O}(t^2/\Delta E)$, we will ignore this contribution. However, it should be noted that the denominator ΔE for this process is proportional to J_S and/or J_L not U , implying of course that we should consider the higher-energy particle and hole multiplets if the strong-coupling limit Eq. (7) is not strictly valid. Note that due to the energy constraint in the effective Hamiltonian the particle and hole are not allowed to annihilate by hopping to the same site. We will ignore the constraint which in three dimensions is expected to give a vanishing contribution to the spectrum at low densities.

1. Charged single-particle excitations

In order to understand charge transport, we need to consider the single-particle and single hole states $|5,l,s\rangle_r\Pi_{r'\neq r}|4\rangle_{r'}$ and $|3,l,s\rangle_r\Pi_{r'}|4\rangle_{r'\neq r}$. Here we have dropped the multiplet indices $(L,S)=(1,\frac{1}{2})$ or $(0,0)$. When acted on by \mathcal{H}_{eff} these excitations are translated to a nearest-neighbor through h with a matrix element

$$\begin{aligned} \langle 4|_r \langle 5,l',s'|_{r'} \left(\sum_{jj',\sigma} t_{jj'}^{rr'} c_{r',j',\sigma}^\dagger c_{r,j,\sigma} \right) | 5,l,s\rangle_r | 4 \rangle_{r'} \\ = \frac{1}{3} \delta_{ss'} t_{l'l'}^{rr'}, \\ \langle 4|_r \langle 3,l',s'|_{r'} \left(\sum_{jj',\sigma} t_{jj'}^{rr'} c_{r,j,\sigma}^\dagger c_{r',j',\sigma} \right) | 3,l,s\rangle_r | 4 \rangle_{r'} \\ = -\frac{2}{3} \delta_{ss'} t_{l'l'}^{rr'}, \end{aligned} \quad (22)$$

and similarly with a factor of $-1/3$ for holes and of $2/3$ for particles with respect to the $n=2$ ground state. The matrix elements in Eq. (22) follow from the explicit expressions for the states

$$|5,1,\frac{1}{2},l,s\rangle = \sqrt{3}c_{ls}^\dagger|4,0,0\rangle,$$

$$|3,1,\frac{1}{2},l,s\rangle = \sqrt{\frac{3}{2}}c_{ls}^\dagger|2,0,0\rangle = \sqrt{\frac{3}{2}}(2s)^{2|l|-1}c_{-l-s}|4,0,0\rangle,$$

$$|1,1,\frac{1}{2},l,s\rangle = c_{ls}^\dagger|0\rangle = \sqrt{3}(2s)^{2|l|-1}c_{-l-s}|2,0,0\rangle, \quad (23)$$

which is a simple exercise in elementary quantum mechanics to derive.

We note the reduced magnitude of the matrix elements compared to the single-particle hopping on empty sites

$$\langle 0|_r \langle 1,l',s|_{r'} \left(\sum_{jj',\sigma} t_{jj',\sigma}^{rr'} c_{r',j',\sigma}^\dagger c_{r,j,\sigma} \right) |1,l,s'\rangle_r |0\rangle_{r'} = \delta_{ss'} t_{ll'}^{rr'}. \quad (24)$$

This is a general result of the reduced Hilbert space due to constraining the n -particle states to the lowest-energy multiplet.

Let us define the particle and hole creation operators

$$c_{5,rls}^\dagger = |5,l,s\rangle_r \langle 4|_r, \quad c_{3,rls}^\dagger = |3,l,s\rangle_r \langle 4|_r, \quad (25)$$

through which the particle and hole states can be written as $c_{5,rls}^\dagger|GS,4\rangle$ and $c_{3,rls}^\dagger|GS,4\rangle$ with $|GS,4\rangle = \Pi_r|4,0,0\rangle_r$. Note that these operators do not obey on-site anticommutation relations, we can only use them with confidence in describing noninteracting single-particle physics.

In terms of these particle and hole operators we now straightforwardly arrive at the following single-particle Hamiltonians for the particle and hole states

$$H_5 = \sum_{\langle rr'\rangle, ll's} \frac{1}{3} t_{ll'}^{rr'} c_{5,rls}^\dagger c_{5,r'l's} + \sum_{r,ls} (9/2U + 3/4J_S + 2J_L - \mu) c_{5,rls}^\dagger c_{5,rls}, \quad (26)$$

$$H_3 = - \sum_{\langle rr'\rangle, ll's} \frac{2}{3} t_{ll'}^{rr'} c_{3,rls}^\dagger c_{3,r'l's} + \sum_{r,ls} (-7/2U + 3/4J_S + 2J_L + \mu) c_{3,rls}^\dagger c_{3,rls}, \quad (27)$$

where the on-site energy is defined with respect to the $E(4,0,0) = 8U - 4\mu$ and where we have introduced the chemical potential μ .

These are just simple tight-binding Hamiltonians which we can diagonalize in momentum space in terms of states

$$|5,k,ls\rangle = c_{5,kl s}^\dagger|GS,4\rangle = \frac{1}{\sqrt{V}} \sum_r e^{i\vec{k}\cdot\vec{r}} c_{5,rls}^\dagger|GS,4\rangle, \\ |3,k,ls\rangle = c_{3,kl s}^\dagger|GS,4\rangle = \frac{1}{\sqrt{V}} \sum_r e^{-i\vec{k}\cdot\vec{r}} c_{3,rls}^\dagger|GS\rangle. \quad (28)$$

In general, these are not eigenstates due to the fact that the hopping is not diagonal in l and we would get three (or more

if there are inequivalent sites) nondegenerate bands depending on the precise nature of the hopping integrals which depend on the crystal symmetry. Quite intriguingly, as seen from Eqs. (26) and (27), the band structure for these particle and hole excitations from the Mott insulating ground state is precisely the noninteracting band structure up to a rescaling factor. The reason for this remarkably simple behavior is that the ground state at even-integer filling is in the trivial ($L=0, S=0$) representations of spin and angular momentum and as such is basically equivalent to the zero-particle vacuum.

2. Mott gap

The Mott gap is defined as the gap between the ground state and the lowest-energy charge-carrying excitation of the insulator. What is often measured, however, is the optical gap as defined by optical conductivity or reflectivity measurements and we will be interested in calculating this too.

The Kubo formula for the optical conductivity which is the short-wavelength limit of the electrical conductivity is at zero temperature

$$\sigma_{aa}(\omega, q=0, T=0) = \frac{2i\hbar^2 e^2}{m^2 V} \sum_m \frac{\omega}{\omega_m} \frac{|\langle m|j^a(q=0)|GS\rangle|^2}{\omega(\omega+i\eta) - \omega_m^2}, \quad (29)$$

where $|m\rangle$ are excited states with $\hbar\omega_m = E_m - E_{GS}$.²² The current operator can be derived from the continuity equation $i\hbar^{-1}[n(r), H] + \nabla \cdot \vec{j}(r)$. For the Hamiltonian Eq. (1) considered here only the tight-binding part contributes and we get

$$\vec{j}(\vec{q}) = \sum_{p, ll's} \left(\frac{\partial}{\hbar \partial \vec{p}} \sum_{\delta} e^{-i\vec{p}\cdot\vec{\delta}} t_{ll'}^{0\delta} \right) c_{p+q, ls}^\dagger c_{p, ll's}, \quad (30)$$

where $\vec{\delta}$ is the set of nearest-neighbor lattice vectors. For a cubic or orthorhombic lattice this simplifies to

$$\vec{j}(\vec{q}) = -\frac{1}{\hbar} \sum_{\vec{p}, ll's, \delta} \delta^a \sin(\vec{p}\cdot\vec{\delta}) t_{ll'}^{0\delta} c_{p+q, ls}^\dagger c_{p, ll's}. \quad (31)$$

The current operator creates particle-hole pairs when acting on the ground state $|GS,4\rangle$ and we expect to get nonzero matrix elements with states

$$|kls, k'l's'\rangle_{p-h} = c_{5,kl s}^\dagger c_{3, k'l's'}^\dagger |GS,4\rangle \quad (32)$$

defined according to Eqs. (28) and (25).

With this we can calculate the matrix element

$$\langle kls, k'l's' |_{p-h} j^a(q=0) |GS\rangle \\ = -\frac{\sqrt{2}}{3\hbar} (2s')^{2|l'|-1} \sum_{\delta} \delta^a \sin(\vec{k}\cdot\vec{\delta}) t_{l, -l'}^0 \delta_{k, k'} \delta_{s, -s'}. \quad (33)$$

Introducing an explicit band structure, i.e., defining $t_{ll'}^{rr'}$, we can in principle calculate the optical conductivity due to

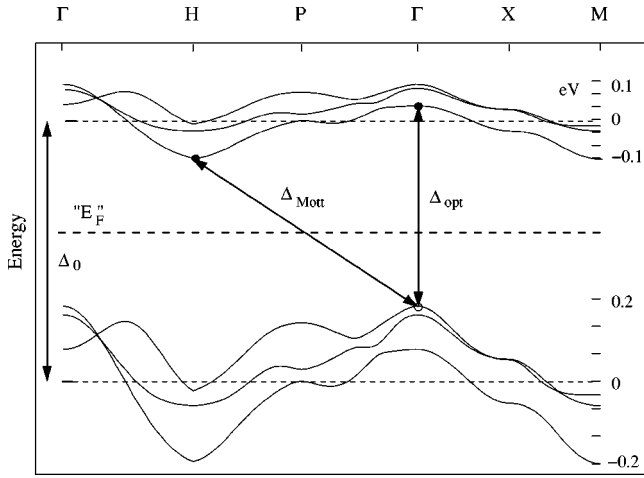


FIG. 2. Sketch of the band structure at doping $n=4$ [K_4C_{60} (Ref. 23)] showing the indirect gap structure with optical gap Δ_{opt} and Mott gap Δ_{Mott} . The thin dashed lines indicate the centers of the particle and hole bands and the energy scales on the right are defined with respect to these. $\Delta_0 = U + 4J_L + \frac{3}{2}J_S$ is the gap in $t=0$ limit.

the particle-hole excitations. A lower bound to the support of the sum in Eq. (29) will tell us the optical gap, below which ω , $\sigma(\omega)$ will decay. We simply maximize the kinetic energy of the particle and hole under the zero-momentum constraint in the usual manner to obtain this. We will ignore the possible complications due to the dispersion and angular momentum part $\sum_{\delta} \delta^{\alpha} \sin(\vec{k} \cdot \vec{\delta}) t_{l,-l'}^{\delta}$, which may kill the matrix elements at some high-symmetry points. Moving slightly away from such symmetry points will give a finite contribution to the response.

The optical gap is thus given by

$$\Delta_{\text{optical}} \geq U + 4J_L + \frac{3}{2}J_S + \left[\frac{1}{3}\varepsilon_i^t(\vec{k}) - \frac{2}{3}\varepsilon_j^t(\vec{k}) \right]_{\min(\vec{k}, i, j)}, \quad (34)$$

where $\varepsilon_j^t(\vec{k})$ is the kinetic energy of the j th band at momentum \vec{k} and $\min(\vec{k}, i, j)$ means minimizing with respect to the momentum and the band indices.

To get the Mott gap we just need to find the lowest-energy particle-hole state, which will in general be smaller than the optical gap. This corresponds to putting the particle at the bottom of the single-particle band and the hole at the top

$$\Delta_{\text{Mott}} = U + 4J_L + \frac{3}{2}J_S + \left[\frac{1}{3}\varepsilon_i^t(\vec{k}) - \frac{2}{3}\varepsilon_j^t(\vec{k}') \right]_{\min(\vec{k}, \vec{k}', i, j)}. \quad (35)$$

In Fig. 2 we present a caricature of the band structure around $n=4$ based on an explicit noninteracting band-structure calculated for K_4C_{60} by Gunnarsson *et al.*,²³ which is rescaled by a factor of 1/3 for the particle band and of 2/3 for the hole band. For this band structure, and any other where the max and min are not at the same \vec{k} vector, we find

an indirect gap where the optical gap is larger than the Mott gap and that the lowest-energy particle-hole excitations have nonzero momentum.²⁴

A word of caution may be appropriate in considering this figure, namely that the single-particle states in the bands are only well defined within our theory for a small density of such states. We depict the lower ‘‘band’’ as filled with single-particle states, but the real entities are only the holes in this band. This is a strongly interacting system and the analogy with a weakly interacting semiconductor has limitations. For instance, it is quite obviously nonsensical to fill up the particle band with a density of more than two particles because that would correspond to a total electron density of more than six. We will return to issue of doping away from the Mott insulator in Sec. IV.

For comparison with other models of the Mott transition on degenerate Hubbard models it is useful to write down a more general expression for the Mott gap. If we make the reasonable assumption that the top and bottom of the band structure are roughly the same magnitude $W/2$, where W is the bandwidth of the tight-binding Hamiltonian h , we can write

$$\Delta_{\text{Mott}} \approx U_{\text{eff}}(4) - \frac{1}{2}W, \quad (36)$$

where $U_{\text{eff}}(4) = U + 4J_L + \frac{3}{2}J_S$. This expression is in sharp contrast to calculations on N -band Hubbard models without the multiplet splitting terms \vec{S}^2 and \vec{L}^2 , where forms such as $\Delta_{\text{Mott}} \approx U - NW$ or $\Delta_{\text{Mott}} \approx U - \sqrt{N}W$ has been suggested.²⁵ The intuitive motivation for the N dependence is an increase in the kinetic energy of the particle-hole state due to the additional hopping channels. In this model we see a different behavior since the number of hopping channels are limited by the strong spin-dependent on-site interactions.

C. Why is $A_3\text{C}_{60}$ metallic?

One of the most striking facts about the fullerides is that the $A_3\text{C}_{60}$ materials are generally metallic given that the even-integer filling materials are likely large- U insulators. The problem of odd-integer filling is significantly more complicated than that of even-integer filling as presented above. The reason for this is that even in the strong-coupling limit, Eq. (7), the ground state consists of states ($n=3, L=1, S=\frac{1}{2}$) with spin and orbital degeneracies. This problem resembles the half-filled single-band Hubbard model with a highly degenerate ground state which will be split to the order of t^2/U . The ground state may then have magnetic and/or orbital orders.

However, if we assume that the putative insulating ground state is not ordered so that the hopping of particles ($n=4, L=0, S=0$) and holes ($n=2, L=0, S=0$) is not frustrated by the spin interactions we can derive a Mott gap in analogous fashion to that for $n=4$ above which reads

$$\begin{aligned}\Delta_{\text{Mott}}(n=3) &\geq U - 4J_L - \frac{3}{2}J_S + \left[\frac{2}{3}\epsilon_i^t(\vec{k}) - \frac{2}{3}\epsilon_j^t(\vec{k}')\right]_{\min(\vec{k}\vec{k}', i, j)} \\ &\approx U_{\text{eff}}(3) - \frac{2}{3}W,\end{aligned}\quad (37)$$

where W again is the noninteracting bandwidth of h . If the ground state has significant magnetic or orbital correlations we expect the gap to be bigger because of a lower-ground-state energy and frustration of the motion of the particle and hole.

Compared to the expression 36 for the Mott gap at $n=4$ we note an increase from $W/2$ to $2W/3$ in the kinetic energy of the particle and holes due to the larger phase-space allowed for hopping. In A_3C_{60} where the bandwidth is around 0.5 eV it appears that this difference will not be large enough to close the 0.5 eV Mott gap seen in A_4C_{60} .

However, in addition there is in this model also a more distinct difference between even- and odd-integer fillings, namely, the sign change of the J_S and J_L terms between the effective Hubbard repulsion $U_{\text{eff}}(4) = U + 4J_L + \frac{3}{2}J_S$ and $U_{\text{eff}}(3) = U - 4J_L - \frac{3}{2}J_S$. This difference comes from the fact that the lowest-energy particle and hole excitations are ($L=0, S=0$) at odd-integer filling, while they are ($L=1, S=\frac{1}{2}$) at even integer. If the multiplet splitting interactions are large enough they could certainly destabilize the Mott insulating ground state at odd-integer filling. For instance, if J_S and J_L are very large such that $U_{\text{eff}}(3) < 0$ and $|U_{\text{eff}}(3)| \gg t$ we would have a spinless Bose liquid consisting of an equal number of two- and four-particle singlets which could only propagate to second order in t .²⁶ At intermediate coupling $U_{\text{eff}}(3) \sim t$ we would expect some correlated metallic state with most of the spectral weight in low spin configurations of the two-, three-, and four-particle states, allowing for hopping to first order in t . Evidence for the formation of singlet configurations on short time scales in the metallic fullerenes $\text{Na}_2\text{CsC}_{60}$, RB_3C_{60} , and the quenched cubic CsC_{60} ($n=1$) have been presented from NMR spin-lattice relaxation measurements.^{27,28}

In addition, we know that A_3C_{60} is quite close to a metal-insulator transition. It has been found that intercalating ammonia into the crystal can cause a transition into an insulating magnetically ordered phase.²⁹ The main effect here is presumably the expansion of the lattice and corresponding decrease in the bandwidth, although the crystal symmetry is also reduced which may be important in facilitating a magnetically ordered ground state. An important consequence of these findings if interpreted through our model is that for A_3C_{60} $U_{\text{eff}}(3) > 0$ because the ground state for small t is magnetic and that $|U_{\text{eff}}(3)| \sim t$ because changes in the magnitude of t can induce a metal-insulator transition.

D. Experiment

A basic observation from experiments is that there appears to be two distinct energy scales in these materials. Probes that are sensitive to spin, in particular NMR, are consistent with a spin gap of around 50–100 meV, while optical conductivity sees a larger charge gap of around 500 meV.

Here we will look at the consistency of the model with these observations and make a fit to estimate our microscopic parameters U , J_L , and J_S .

1. Optical gap

The charge gap is seen in optical conductivity as a depletion of the low-energy weight in K_4C_{60} and Rb_4C_{60} below roughly 500 meV.⁴ By inspection of Fig. 2 together with expression (34) for the optical gap we get the following estimate

$$\Delta_{\text{opt}}(\text{K}_4\text{C}_{60}) \approx U_{\text{eff}}(4) - 200 \text{ meV} \approx 500 \text{ meV}, \quad (38)$$

where again $U_{\text{eff}}(4) = U + 4J_L + \frac{3}{2}J_S$. Solving Eq. (38) gives $U_{\text{eff}}(4) \approx 700 \text{ meV}$.

We can compare this to A_3C_{60} where we expect the charge gap to close. Using expression (37) for the charge gap at $n=3$ together with a bare bandwidth of 600 meV gives

$$\Delta_{\text{Mott}}(A_3C_{60}) \approx U_{\text{eff}}(3) - 400 \text{ meV} \leq 0, \quad (39)$$

with $U_{\text{eff}}(3) = U - 4J_L - \frac{3}{2}J_S$. Together with the estimate $U_{\text{eff}}(3) > 0$ as discussed in Sec. III C we thus find the rough estimate of $0 < U_{\text{eff}}(3) \leq 400 \text{ meV}$.

Combining the values for $U_{\text{eff}}(4)$ and $U_{\text{eff}}(3)$ we can now estimate the microscopic parameters of the model. We find $U \leq 550 \text{ meV}$ and $150 \text{ meV} \leq \frac{3}{2}J_S + 4J_L < 350 \text{ meV}$.

2. NMR, $1/T_1$

Various probes^{5,6} have detected a thermally activated magnetic susceptibility in K_4C_{60} and Rb_4C_{60} and more recently also in Na_2C_{60} .³⁰ This has been interpreted as evidence for a singlet-triplet gap of Jahn-Teller distorted molecules, where a molecule is thermally excited from the JT ground-state singlet to the triplet which then acts as a local moment. In the model presented here it is natural to assign such experimental signatures of gapped spin excitations to the spin modes or magnons which are a necessary part of the spectrum of the nonmagnetic Mott insulator.

We will be focusing on measurements of $1/T_1$, the spin-lattice relaxation rate, deriving the temperature dependence of the relaxation by the magnons in the limit $T \ll \Delta_s$.

The probability of a transition between nuclear spin states with z component $m' = m \pm 1$ due to a two magnon process which scatters a magnon with $i = (L^z, S^z)$ and momentum k to $i' = (L'^z, S'^z)$ and k' is given by Fermi's golden rule as

$$\begin{aligned}W_{mm'} &= \sum_{ik, i'k'} \frac{2\pi}{\hbar} |\langle m, n_{ik}, n'_{i'k'} | V | m', n_{ik} - 1, n'_{i'k'} + 1 \rangle|^2 \\ &\times \delta(E_{ik} - E_{i'k'}),\end{aligned}\quad (40)$$

where n_{ik} is the magnon number operator, the interaction $V = A\vec{I} \cdot \vec{S}_0$ with hyperfine coupling A , nuclear spin \vec{I} and electron spin at the nuclear site \vec{S}_0 . We have dropped the small, typically $\sim 10^{-6}$ eV, Zeeman splitting of the nuclear spin.

The electron-spin operator will act as a $b_{r, L^z S^z}^\dagger + (m - m') b_{r, L^z S^z}$ with some small prefactor given by the overlap of these states with the single atom, where $b_{r, L^z S^z}^\dagger$

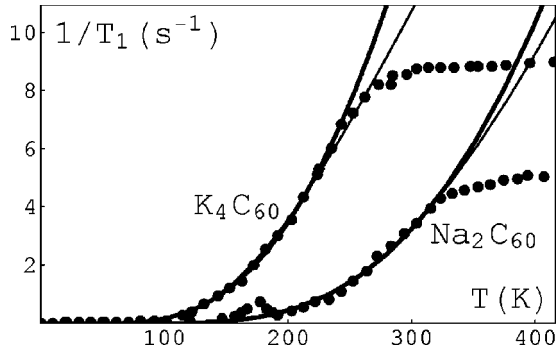


FIG. 3. Fit to ^{13}C NMR data by Brouet *et al.* (Ref. 30). The thick lines are fits to $1/T_1 \sim T^2 e^{-\Delta_s/T}$ with $\Delta_s = 240$ K for K_4C_{60} and $\Delta_s = 710$ K for Na_2C_{60} . The thin lines are fits to $1/T_1 \sim e^{-\Delta_s/T}$ with corresponding $\Delta_s = 660$ K and 1260 K. (The bump around 180 K for Na_2C_{60} is presumably a molecular motion peak.)

creates a triplet excitation. Ignoring the details of the matrix element between the different triplet states one finds that the general magnon matrix element is given by $\langle n_{i'k'} + 1 \rangle \times \langle n_{ik} \rangle$, where $\langle n_{ik} \rangle = (e^{\beta E_{ik}} - 1)^{-1}$ is just the Bose occupation of the magnons. Finally the relaxation rate is given by³¹ $\frac{1}{2} \sum_{mm'} W_{mm'} (E_m - E_{m'})^2 / \sum_m E_m^2$ where the magnon part of $W_{mm'}$ clearly is independent of m and m' . We thus arrive at the final expression

$$1/T_1 \sim \int_{\Delta_s}^{\Delta_s + W_{\text{mag}}} d\epsilon \frac{N^2(\epsilon)}{\sinh^2(\beta\epsilon/2)}, \quad (41)$$

where we have converted the sums to integrals by introducing the density of magnon states $N(\epsilon)$. Here Δ_s is the spin gap, i.e., the lower edge of the magnon band, and W_{mag} is the magnon bandwidth.

For $T \ll \Delta_s$ we can replace the $1/\sinh^2(\beta\epsilon/2)$ by $4e^{-\beta\epsilon}$ and the integral is dominated by $\epsilon \sim \Delta_s$. Assuming a quadratic dispersion at the band edge we get $N(\epsilon) \sim \sqrt{\epsilon - \Delta_s}$ for $\epsilon \gtrsim \Delta_s$. By change of integration variable we arrive at the temperature dependence

$$1/T_1 \sim T^2 e^{-\Delta_s/T}, \quad T \ll \Delta_s. \quad (42)$$

Figure 3 shows a fit of this model to ^{13}C $1/T_1$ data on K_4C_{60} and Na_2C_{60} .³⁰

We get an excellent fit to the below room-temperature activated behavior with a value $\Delta_s = 240$ K ≈ 25 meV for K_4C_{60} . For comparison we also show fits to a model of localized triplet states corresponding to $W_{\text{mag}} = 0$ and $1/T_1 \sim e^{-\Delta_s/T}$. This is the fit used in the the experimental work^{5,6,30} which is based on a model of a static uniform Jahn-Teller singlet-triplet gap. In this intermediate temperature regime it is difficult to tell which fit is best, in particular considering the fact that both models clearly fail at higher temperatures where the relaxation rapidly saturates, and we conclude that these NMR data cannot resolve the two scenarios.

Nevertheless, using the value $\Delta_s = 25$ meV for the spin gap we may estimate the microscopic parameters. Given a bandwidth W_{mag} which we assume to be symmetric around the center we get

$$\Delta_s = \bar{\Delta} - W_{\text{mag}}/2, \quad (43)$$

where $\bar{\Delta} = 2J_L + 2J_S$ is the $t=0$ spin gap. (There is an additional corrections to the spin gap of the order of t^2/U which is a shift of the ground-state energy which should be included in a more rigorous treatment.) A very rough estimate of the bandwidth may be given by the degeneracy of the spin modes $W_{\text{mag}} = 9t^2/U$. With $U \approx 500$ meV as derived from charge gap and taking $t \approx 100$ meV from band-structure calculations gives $W_{\text{mag}} \approx 200$ meV. Collecting into Eq. (43) for the spin gap gives $\bar{\Delta} = 2J_L + 2J_S \approx 125$ meV, which seems in reasonable agreement with the estimate $150 \text{ meV} \approx \frac{3}{2}J_S + 4J_L < 350$ meV from the charge gap. This order of magnitude agreement for the coupling constants J_S and J_L is certainly encouraging in that it comes from experiments on two apparently separate physical quantities.

A fit to $1/T_1$ for Na_2C_{60} gives a larger gap of around 700 K. Within our model the $t=0$ spin gap $\bar{\Delta}$ is the same for $n=2$ and $n=4$ so the differing spin gaps are somewhat unexpected. However, since the crystal structure is different, the tight-binding Hamiltonians of these materials may be very different and consequently the bandwidth of the spin modes. In fact, Na_2C_{60} is fcc while K_4 and Rb_4 are body-centered tetragonal. The natural interpretation for the variations within this model is thus variations of the magnon bandwidth. Along the same lines we note the behavior of $1/T_1$ in Rb_4C_{60} under pressure where it is found that the activated behavior is replaced or coexists with a nonactivated component related to gapless excitations.⁶ It has been suggested that this is related to a closing of the Mott gap due to the expected pressure induced increase of the bare bandwidth. Within our model we find a possible alternative interpretation in terms of a closing of the spin gap.

Above room temperature the activated behavior stops and the relaxation rate saturates. Within our simple noninteracting model for the spin modes we cannot expect to be able to address the high-temperature behavior when a significant number of modes are excited. A more sophisticated treatment requires us to properly account for the interactions between the spin modes as well as the exclusion statistics that are ignored in the single-particle picture. The saturation could also be related to molecular degrees of freedom at higher temperatures, which are completely neglected in our model.³⁰ However, we note that this rapid saturation is very reminiscent of the behavior of $1/T_1$ in spin ladder materials with gapped magnons,³² where it is believed to have a purely electronic origin.³³

IV. THE DOPED MOTT INSULATOR

We will now look at the problem of an incommensurate particle density away from the Mott insulators at even-integer filling $n=2$ and $n=4$. This is obviously a much

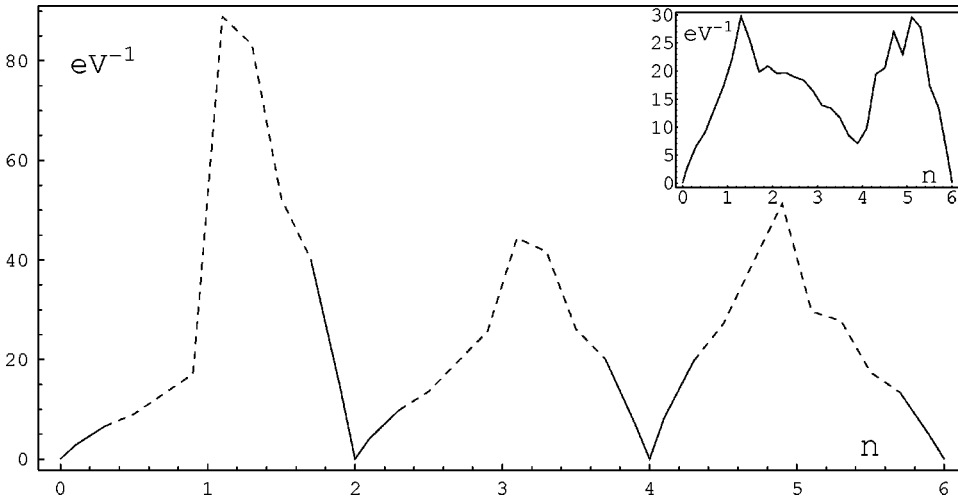


FIG. 4. Density of states (both spins) as function of filling n given the noninteracting DOS inset. The dashed lines are extrapolations of Eq. (44) toward odd-integer filling. The noninteracting DOS is calculated from the band structure of unidirectional A_3C_{60} (Ref. 20).

more difficult task because in the strong-coupling limit the ground state will be highly degenerate. As a concrete example, at a doping $n=2+x$ ($x<1$) the ground state at $t=0$ is the set of states with x three-particle states $(3,1,\frac{1}{2})$ and $(1-x)$ two-particle states $(2,0,0)$ at arbitrary positions in space. Introducing t by means of effective Hamiltonian (17) we find to first order in t nearest-neighbor interchange of the two- and three-particle states and to second order in t spin and orbital exchange terms between nearest-neighbor three-particle states. This can be described by a generalized t - J model including a no double occupancy constraint because only two and three-particle states are allowed.

At first glance this may appear to be an even more difficult problem than that of a doped antiferromagnet because of the additional orbital degrees of freedom. However, in the low-density limit, $x\ll 1$, it is in fact considerably simpler than the doped antiferromagnet because only the doped particles (or holes) have internal spin and orbital degrees of freedom. In the doped antiferromagnet the scenario is just the opposite with a large number $1-x$ of spinful particles and a small number x of spinless holes. This of course gives rise to the very complex behavior in such systems where the spin interactions J can compete with the hopping t even in the limit $J\sim t^2/U\ll t$ because the important energetics is given roughly by xt and $(1-x)J$. Here for the doped nonmagnetic Mott insulator a similar consideration would lead us to compare xJ with xt because it is the doped particles or holes that carry both the spin and momentum. Effectively we are thus looking at the low-density (heavily doped) limit of a t - J model.

We will completely neglect the nearest-neighbor exchange interactions as well as the no double occupancy constraint and only consider the single-particle physics. Certainly, for the problem of a single-particle or hole doped into the nonmagnetic Mott insulator this is completely rigorous and again in sharp contrast to the problem of a single hole in an antiferromagnet where interactions obviously cannot be neglected. Even this single-particle physics has some interesting implications for the doping dependence in the metallic fullerenes.

A. Small Fermi surface

The problem of a single-particle or hole was addressed already in Sec. III B 1 in connection with particle-hole excitation. There we showed that the single-particle or hole spectra are equivalent to the noninteracting $H_I=0$ spectrum up to a rescaling by a factor of $1/3$ or $2/3$. At least in the very low-density limit, $n=2+x$ or $n=4+x$ with $|x|\ll 1$, we expect these single-particle states to give a qualitatively accurate picture by filling x such states.

In particular this implies a “small Fermi surface,” where the number of delocalized charge carriers is proportional to the number of doped holes or particles x and not the total filling n . The remaining degrees of freedom are frozen below the Mott gap. One important consequence is that the density of states at the Fermi surface for small doping x will be given by the density of states (DOS) at the band edges of the noninteracting problem by the simple relation

$$\text{DOS}_{\text{strong coupling}}(n=2-x) \approx 3 \text{DOS}_{\text{noninteracting}}(n=6-x),$$

$$\text{DOS}_{\text{strong coupling}}(n=2+x) \approx 3/2 \text{DOS}_{\text{noninteracting}}(n=x),$$

$$\text{DOS}_{\text{strong coupling}}(n=4-x) \approx 3/2 \text{DOS}_{\text{noninteracting}}(n=6-x),$$

$$\text{DOS}_{\text{strong coupling}}(n=4+x) \approx 3 \text{DOS}_{\text{noninteracting}}(n=x),$$

$$x\ll 1. \quad (44)$$

A detailed picture of what happens at larger doping $x\rightarrow 1$ as we approach odd-integer filling is beyond our methods. However, a naive extrapolation of the results valid for small x all the way to $x=1$ gives a density of states as shown in Fig. 4, where the density of states is generally peaked at odd-integer filling as a consequence of the rapid decay toward the effective band edges at even-integer filling. For reasons discussed in Sec. III C we have to be in an intermediate coupling regime, where the system is metallic at odd-integer filling for this extrapolation to have any credibility.

There is an interesting experiment that corroborates the small Fermi-surface picture in C_{60} which is the variation of density of states in $\text{Na}_2\text{Cs}_x\text{C}_{60}$ ($0<x<1$) corresponding to a doping range $2<n<3$.⁷ It was estimated from the Pauli sus-

ceptibility that for samples with $n=2.25, 2.5, 2.75, 3$ the density of states varies as 5, 7, 11, 15 eV^{-1} (both spins). Correspondingly, T_c drops rapidly from 12 K at $n=3$ to 7 K at $n=2.75$ and to $<0.5\text{K}$ at $n=2.5$. Certainly, this behavior seems consistent with the scenario sketched in Fig. 4, where the density of states drops rapidly as the effective Hubbard band edges are approached at even-integer filling.

The failure of naive band theory in the presence of strong local repulsion is a consequence of the large inherent charge fluctuations of such an uncorrelated state of delocalized electrons. It may be illuminating to recall some of Hubbard's original work on the topic of narrow-band systems.³⁴ For an m -fold degenerate band at filling n the probability $P_N(m, n)$ of having N electrons on a particular atom (molecule) is given by

$$P_N(m, n) = \binom{m}{N} \left(\frac{n}{m} \right)^N \left(1 - \frac{n}{m} \right)^{m-N}, \quad (45)$$

where $\binom{m}{N}$ is the multiplicity of atomic states with N particles. The rms fluctuation is given by $(\Delta_N)_{\text{rms}} = \sqrt{n(1-n/m)}$, which has a maximum $(\Delta_N)_{\text{rms}} = \sqrt{m/2}$ at half filling $n=m/2$. Clearly, at finite doping there are significant charge fluctuations of the order 1 which cost an energy of the order of U per site in an uncorrelated state and which grows with the degeneracy. We can get an estimate of the energy cost of the charge fluctuations for our model by comparing the potential energy $E = \langle H_I \rangle$ in an uncorrelated state which is the ground state of the kinetic energy h with that given by the small Fermi-surface state which is the ground state of the potential energy H_I . The latter is at filling n given by p_N N -particle states and p_{N+1} $N+1$ -particle states in the lowest energy multiplet where $N \leq n < N+1$ and $p_N N + p_{N+1}(N+1) = n$. The potential energy of this state is given by

$$\langle H_I \rangle_{\text{corr}} = p_N E_0(N) + p_{N+1} E_0(N+1), \quad (46)$$

where $E_0(N)$ is the energy of the ground-state multiplet with N particles. Expression (45) turns into

$$P_{N,L,S}(n) = (2L+1)(2S+1) \left(\frac{n}{6} \right)^N \left(1 - \frac{n}{6} \right)^{6-N} \quad (47)$$

for this model, where the N -particle multiplets are split according to L and S and the corresponding potential energy for the uncorrelated state is

$$\langle H_I \rangle_{\text{uncorr}} = \sum_{N,L,S} P_{N,L,S}(n) E(N, L, S). \quad (48)$$

Figure 5 shows $\Delta E = \langle H_I \rangle_{\text{uncorr}} - \langle H_I \rangle_{\text{corr}}$ as a function of doping and in units of $U_{\text{eff}}(2) = U_{\text{eff}}(4) = U + 4J_L + 3/2J_S$ for two cases $J_L = J_S = 0$ and $J_L = 0.1U, J_S = 0.2U$.

We see that in a wide doping range around half filling there is a significant energy cost due to charge fluctuations in an uncorrelated state. Given that this leads to the Mott insulating behavior at even-integer filling we would also expect significant correlation effects in the metallic regions $2 < n < 4$, consistent with the small Fermi-surface scenario.

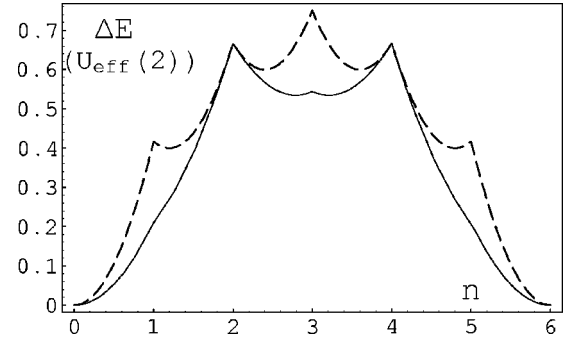


FIG. 5. Potential-energy difference, in units of $U_{\text{eff}}(2) = U + 4J_L + 3/2J_S$, between an uncorrelated and correlated ground state as a function of filling n . The solid line is for $J_S = 2J_L = 0.1U$ and the dashed line for $J_L = J_S = 0$.

Hubbard's treatment of narrow-band systems used a real-space Greens function method which is exact in the zero bandwidth $t=0$ case but which depends critically on neglecting correlations between electrons on different atoms in the finite bandwidth case. He found that in the narrow bandwidth limit the original noninteracting band splits into a large number of bands which correspond to transitions between states with particle number differing by one. In addition these Hubbard bands reflect the noninteracting band with density of states which are some functional of the noninteracting density of states. Our result for the doped Mott insulator is essentially a special case of Hubbard's results for which we can solve for the quasiparticle spectrum exactly in the low-density limit where we can neglect interactions between the doped particles or holes.

B. High Temperatures

In the preceding section we discussed the ground-state properties of the doped Mott insulator close to even-integer filling. We found a band of single-particle states which up to a rescaled hopping are equivalent to the states of the non-interacting problem. At low temperatures we thus expect a simple metallic behavior with bandlike charge transport. Here we will speculate on some of the interesting physics which could emerge from the model at higher temperatures.

The derivation of the single-particle Hamiltonians, Eqs. (26) and (27), for the particle and hole states depends crucially on the fact that the Mott insulating ground state is of the simple nondegenerate form $|GS, 4/2\rangle = \prod_r |n=4/2, L=0, S=0\rangle_r$ and that we can ignore the higher orbital and spin multiplets in the two and four-particle molecular spectra. At elevated temperatures of the order the the spin gap Δ_s this assumption is no longer justified as the the spin and angular momentum modes discussed in Sec. III A are thermally occupied and we should consider their effect on the quasiparticle states. [The activated behavior discussed in Sec. III D 2 which has been linked to gapped triplet excitations is seen in NMR ($1/T_1$) also in the metallic $\text{Na}_2\text{CsC}_{60}$ and Rb_3C_{60} (Ref. 27).] These, in fact, interact very strongly with the quasiparticles in a quite nontrivial fashion. In the presence of such an excited spin or orbital state the nearest-

neighbor hopping integrals described by Eq. (22) turn into some more complicated expressions given by, for instance,

$$\begin{aligned} & \langle 4,1,1,L'^z,S'^z|_r \langle 3,l',s'|_r \\ & \times \left(\sum_{jj',\sigma} t_{jj'}^{rr'} c_{r,j,\sigma}^\dagger c_{r',j',\sigma} \right) |3,l,s\rangle_r |4,1,1,L^z,S^z\rangle_{r'}, \end{aligned} \quad (49)$$

in the case of a hole hopping to a site occupied by a spin triplet. Depending on the configurations of the spin triplet states the hopping of the hole ($|3,l,s\rangle$) may be completely suppressed or it may require a spin flip. Certainly the nearest-neighbor hopping integrals would be completely altered from the simple form of Eq. (22).

It is not obvious how to model this problem but the most naive scenario might be to ignore the hopping of the spin and orbital states and replace them by thermally excited impurities causing disorder in the hopping of the particles or holes. Such a model would be similar to that suggested by Varma to explain the paramagnetic insulator to ferromagnetic metal transition in lanthanum manganites (giant magnetoresistive compounds).³⁵

One may speculate that this temperature activated off-diagonal disorder could destroy the bandlike motion of the charge carriers and possibly be related to anomalous properties of A_3C_{60} at elevated temperatures such as the evidence for localization from NMR,²⁷ the disappearance of the Fermi edge³⁶ and the nonsaturation of resistivity and the corresponding extremely short mean-free paths.³⁷

V. CONCLUSIONS

We have studied an orbitally degenerate three-band Hubbard model with additional multiplet splitting on-site interactions $J_S \vec{S}^2$ and $J_L \vec{L}^2$ which favor low-spin and low-orbital angular momentum. We use the effective Hamiltonian method in the strong-coupling limit $U \gg J_S \gg J_L \gg t$ perturbatively to second order in t . At even-integer filling, $n=2$ or $n=4$, this model is an insulator with a nondegenerate ground state where the electrons at each site occupy the $L=0$ and $S=0$ configurations and with distinct spin and charge gaps. The trivial ground state allows for a simple single-particle description of spin and charge excitations. The lowest-energy spinful excitations is a band of magnons with a bandwidth $W_{\text{mag}} \sim t^2/U$ and a gap $\Delta_s = 2J_L + 2J_S - \mathcal{O}(t^2/U)$. A single-particle or hole doped into the Mott insulator are described by the noninteracting tight-binding Hamiltonian but with an overall rescaling by a factor of $1/3$ or $2/3$ of the hopping integrals and corresponding bandwidth. The latter allows for a detailed description of the particle-hole excitations and the corresponding charge gap is given by $\Delta_{\text{Mott}} \approx U + 4J_L + 3/2J_S - W/2$ in terms of the bandwidth W of the noninteracting Hamiltonian.

Close to the Mott insulator, at filling $2+x$ or $4+x$ with $|x| \ll 1$, we find a metallic state with a “small Fermi surface,” where the density of charge carriers is given by $|x|$ and a density of states which is simply a renormalization by a factor of 3 or $3/2$ of the density of states at the band edges

of the noninteracting band structure. Consequently, in three dimensions the density of states will in general increase rapidly with the doping x .

In this model there is also a distinct difference between even- and odd-integer fillings, which follows from the simple fact that an odd number of electrons cannot form a spin singlet. From this follows that the effective on-site repulsion is given by $U_{\text{eff}}(n=2/4) = U + 4J_L + 3/2J_S$ at even-integer filling and by $U_{\text{eff}}(n=1/3/5) = U - 4J_L - 3/2J_S$ at odd. Consequently, depending on the magnitude of J_L and J_S , the Mott gap may be significantly reduced or vanish at odd-integer filling.

The properties of this model are strikingly similar to the phenomenology of the fullerides A_nC_{60} with $2 \leq n \leq 4$. The nonmagnetic Mott insulator at even-integer filling with a small spin gap and a larger charge gap, the even/odd effect at integer doping where A_3C_{60} is generally metallic, as well as the rapid suppression of the DOS and the corresponding superconducting transition temperatures as the filling approaches even integer. We do a fit of the model to the charge gap from optical conductivity and the spin gap from NMR $1/T_1$ in K_4C_{60} which appear consistent with values of J_S and J_L of around 50–100 meV.

There is a number of interesting open questions about the model and the possible implications to alkali doped C_{60} . In particular, we need a better understanding of the physics at odd-integer filling on the metallic side of the Mott transition. Can this state have a superconducting ground state even though, as evidence suggests, $U_{\text{eff}}(3) > 0$ such that there is no bare attraction in the way envisioned by Chakravarty and coworkers as an electronic mechanism of superconductivity? In fact, also at even-integer filling there have been intriguing suggestions of an intermediate superconducting state in the metal-insulator transition.^{16,17} Another issue is the properties of the model at elevated temperatures approaching the spin gap, where we have found that the spin and orbital modes interact strongly with the charge carriers and may significantly affect the simple bandlike charge transport.

APPENDIX: SECOND-ORDER CANONICAL TRANSFORMATION

Here we derive the expressions for the second-order terms in the effective Hamiltonian Eq. (17). Starting with Eq. (15)

$$\mathcal{H}_{\text{eff}} = H_I + h^0 + i[\mathcal{S}_1, h^0] + \frac{i}{2}[\mathcal{S}_1, h^1] + i[\mathcal{S}_2, H_I],$$

where \mathcal{S}_1 is given by

$$\mathcal{S}_1 = \sum_{\langle r,r' \rangle} \frac{ih_{ab}^{1,rr'}}{E(b) - E(a)} |a\rangle_{rr'} \langle b|_{rr'}. \quad (\text{A1})$$

Our purpose is to construct \mathcal{S}_2 such that it cancels terms which connect different energy subsectors from the commutators $[\mathcal{S}_1, h^{0/1}]$. We have

$$\begin{aligned}
i[\mathcal{S}_1, h^{0/1}] &= - \sum_{\langle r, r' \rangle, \langle r'', r''' \rangle} \frac{h_{ab}^{1,rr'}}{E(b) - E(a)} \\
&\quad \times h_{cd}^{0/1, r'' r'''} [|a\rangle_{rr'} \langle b|_{rr'}, |c\rangle_{r'' r'''} \langle d|_{r'' r'''}] \\
&= - \sum_{\langle r, r' \rangle} \frac{h_{ab}^{1,rr'}}{E(b) - E(a)} \\
&\quad \times h_{cd}^{0/1, rr'} [|a\rangle_{rr'} \langle b|_{rr'}, |c\rangle_{rr'} \langle d|_{rr'}] \\
&\quad - \sum_{\langle r, r', r'' \rangle} \frac{h_{ab}^{1,rr'}}{E(b) - E(a)} \\
&\quad \times h_{cd}^{0/1, r' r''} [|a\rangle_{rr'} \langle b|_{rr'}, |c\rangle_{r' r''} \langle d|_{r' r''}], \tag{A2}
\end{aligned}$$

where we have used the fact that the operators commute if there is no overlap between sites. Using the complete set of three site states $1 = \Pi_a |a\rangle_{rr'} \langle a|_{rr'}$ for the three-site interaction we arrive at

$$\begin{aligned}
i[\mathcal{S}_1, h^{0/1}] &= - \sum_{\langle r, r' \rangle, c} \left(\frac{h_{ac}^{1,rr'}}{E(c) - E(a)} h_{cb}^{0/1, rr'} \right. \\
&\quad \left. + h_{ac}^{0/1, rr'} \frac{h_{cb}^{1,rr'}}{E(c) - E(b)} \right) |a\rangle_{rr'} \langle b|_{rr'} \\
&\quad - \sum_{\langle r, r', r'' \rangle, c} \left(\frac{h_{ac}^{1,rr'}}{E(c) - E(a)} h_{cb}^{0/1, r' r''} \right. \\
&\quad \left. + h_{ac}^{0/1, r' r''} \frac{h_{cb}^{1,rr'}}{E(c) - E(b)} \right) |a\rangle_{rr' r''} \langle b|_{rr' r''}. \tag{A3}
\end{aligned}$$

We now split this into a part $\delta_{E(a)E(b)}$ which is diagonal in energy and $(1 - \delta_{E(a)E(b)})$ which connects different energy sectors. The latter part we can cancel by solving for \mathcal{S}_2 , schematically

$$[\mathcal{S}_2, H_I] = - \left([\mathcal{S}_1, h^0] + \frac{1}{2} [\mathcal{S}_1, h^1] \right)_{\text{off-diagonal}}. \tag{A4}$$

Using an ansatz $\mathcal{S}_2 = \sum_{\langle r, r' \rangle} \mathcal{S}_{2,ab}^{r r'} |a\rangle_{rr'} \langle b|_{rr'} + \sum_{\langle r, r', r'' \rangle} \mathcal{S}_{2,ab}^{r r' r''} |a\rangle_{rr' r''} \langle b|_{rr' r''}$ and using the fact that $[[a\rangle_{rr' r''} \langle b|_{rr' r''}, H_I] = [E(b) - E(a)] |a\rangle_{rr' r''} \langle b|_{rr' r''}$, we can solve for $\mathcal{S}_2 \sim \mathcal{O}(t^2/\Delta E)$. Apart from the cancellation, \mathcal{S}_2 will only contribute to higher orders.

Having done the cancellation we are left with terms that are diagonal in energy. Clearly $[\mathcal{S}_1, h^0]$ does not contribute to this because h^0 is diagonal in energy and $\mathcal{S} \sim h^1$ is strictly off diagonal. The result for the remaining second order terms is

$$\begin{aligned}
\frac{i}{2} [\mathcal{S}_1, h^1]_{\text{diagonal}} &= - \frac{1}{2} \sum_{\langle r, r' \rangle, c} \frac{h_{ac}^{1,rr'} h_{cb}^{1,rr'} + h_{ac}^{1,rr'} h_{cb}^{1,rr'}}{E(c) - E(a)} \\
&\quad \times \delta_{E(a)E(b)} |a\rangle_{rr'} \langle b|_{rr'} \\
&\quad - \frac{1}{2} \sum_{\langle r, r', r'' \rangle, c} \frac{h_{ac}^{1,rr'} h_{cb}^{1, r' r''} + h_{ac}^{1, r' r''} h_{cb}^{1,rr'}}{E(c) - E(a)} \\
&\quad \times \delta_{E(a)E(b)} |a\rangle_{rr' r''} \langle b|_{rr' r''}, \tag{A5}
\end{aligned}$$

which simplifies to the final expression given in Eq. (17).

*Electronic address: mgranath@fy.chalmers.se

†Electronic address: ostlund@fy.chalmers.se

¹S. Sachdev, Ann. Phys. (N.Y.) **303**, 226 (2003).

²We use the term Mott insulator in the broad context of an insulator, which according to band theory calculations should be a metal because there is at least one partially filled band. However, we will primarily consider even-integer filling which could correspond to a band insulator because there is an even number of electrons per unit cell. A more distinct definition of a Mott insulator valid in our case is an insulator in which the electronic charge gap and spin gap are different.

³For a review see O. Gunnarsson, Rev. Mod. Phys. **69**, 575 (1997).

⁴Y. Iwasa and T. Kaneyasu, Phys. Rev. B **51**, 3678 (1995); M. Knupfer and J. Fink, Phys. Rev. Lett. **79**, 2714 (1997).

⁵I. Lukyanchuk, N. Kirova, F. Rachdi, C. Goze, P. Molinie, and M. Mehring, Phys. Rev. B **51**, 3978 (1995); G. Zimmer, M. Mehring, C. Goze, and F. Rachdi, *ibid.* **52**, 13300 (1995).

⁶R. Kerkoud, P. Auban-Senzier, D. Jérôme, S. Brazovskii, I. Lukyanchuk, N. Kirova, F. Rachid, and C. Goze, J. Phys. Chem. Solids **57**, 143 (1996).

⁷T. Yildirim, L. Barbedette, J.E. Fischer, C.L. Lin, J. Robert, P.

Petit, and T.T.M. Palstra, Phys. Rev. Lett. **77**, 167 (1996).

⁸N. Manini, E. Tosatti, and A. Auerbach, Phys. Rev. B **49**, 13 008 (1994).

⁹C.A. Kuntscher, G.M. Bendele, and P.W. Stephens, Phys. Rev. B **55**, 3366 (1997).

¹⁰S. Chakravarty, M.P. Gelfand, and S.A. Kivelson, Science **254**, 970 (1991).

¹¹G. Baskaran and E. Tosatti, Curr. Sci. **61**, 33 (1991).

¹²For a discussion of Hund's rules and violations of them, see W. Kutzelnigg and J.D. Morgan III, Z. Phys. D: At., Mol. Clusters **36**, 197 (1996).

¹³S.R. White, S. Chakravarty, M.P. Gelfand, and S.A. Kivelson, Phys. Rev. B **45**, 5062 (1992).

¹⁴M. Fabrizio and E. Tosatti, Phys. Rev. B **55**, 13 465 (1997).

¹⁵M. Capone, M. Fabrizio, P. Giannozzi, and E. Tosatti, Phys. Rev. B **62**, 7619 (2000).

¹⁶M. Capone, M. Fabrizio, and E. Tosatti, Phys. Rev. Lett. **86**, 5361 (2001).

¹⁷M. Capone, M. Fabrizio, C. Castellani, and E. Tosatti, Science **296**, 2364 (2002).

¹⁸M. Lüders, A. Bordonni, N. Manini, A. DalCorso, M. Fabrizio, and

- E. Tosatti, *Philos. Mag.* B **82**, 1611 (2002).
- ¹⁹P.E. Lammert, D.S. Rokhsar, S. Chakravarty, S. Kivelson, and M.I. Salkola, *Phys. Rev. Lett.* **74**, 996 (1995).
- ²⁰N. Laouini, O.K. Andersen, and O. Gunnarsson, *Phys. Rev. B* **51**, 17 446 (1995).
- ²¹P. Fazekas, *Lecture Notes on Electron Correlation and Magnetism* (World Scientific, Singapore, 1999).
- ²²G. D. Mahan, *Many-Particle Physics*, 2nd ed. (Plenum Press, New York, 1990).
- ²³O. Gunnarsson, S.C. Erwin, E. Koch, and R.M. Martin, *Phys. Rev. B* **57**, 2159 (1998).
- ²⁴For a review on semiconductors with indirect gaps, see B. I. Halperin and T. M. Rice, in *Solid States Physics*, edited by F. Seitz, D. Turnbull, and H. Ehrenreich (Academic, New York, 1968), Vol. 21.
- ²⁵J.P. Lu, *Phys. Rev. B* **49**, 5687 (1994); O. Gunnarsson, E. Koch, and R.M. Martin, *ibid.* **54**, 11 026 (1996).
- ²⁶S. Chakravarty and S.A. Kivelson, *Phys. Rev. B* **64**, 064511 (2001).
- ²⁷V. Brouet, H. Alloul, S. Garaj, and L. Forró, *Phys. Rev. B* **66**, 155124 (2002).
- ²⁸V. Brouet, H. Alloul, and L. Forró, *Phys. Rev. B* **66**, 155123 (2002).
- ²⁹Y. Iwasa, H. Shimoda, T.T.M. Palstra, Y. Maniwa, O. Zhou, and T. Mitani, *Phys. Rev. B* **53**, 8836 (1996); T. Takenobu, T. Muro, Y. Iwasa, and T. Mitani, *Phys. Rev. Lett.* **85**, 381 (2000).
- ³⁰V. Brouet, H. Alloul, L. Thien-Nga, S. Garaj, and L. Forró, *Phys. Rev. Lett.* **86**, 4680 (2001); V. Brouet, H. Alloul, S. Garaj, and L. Forró, *Phys. Rev. B* **66**, 155122 (2002).
- ³¹C. P. Slichter, *Principles of Magnetic Resonance* (Springer, New York, 1990).
- ³²T. Imai, K.R. Thurber, K.M. Shen, A.W. Hunt, and F.C. Chou, *Phys. Rev. Lett.* **81**, 220 (1998); Y. Piskunov, D. Jérôme, P. Auban-Senzier, P. Wzietek, C. Bourbonnais, U. Ammerhal, G. Dhalenne, and A. Revcolevschi, *Eur. Phys. J. B* **24**, 443 (2001).
- ³³D.A. Ivanov and P.A. Lee, *Phys. Rev. B* **59**, 4803 (1999).
- ³⁴J. Hubbard, *Proc. R. Soc. London, Ser. A* **276**, 238 (1963); *ibid.* **277**, 237 (1964).
- ³⁵C.M. Varma, *Phys. Rev. B* **54**, 7328 (1996).
- ³⁶M. Knupfer, M. Merkel, M.S. Golden, J. Fink, O. Gunnarsson, and V.P. Antropov, *Phys. Rev. B* **47**, 13 944 (1993).
- ³⁷A.F. Hebard, T.T.M. Palstra, R.C. Haddon, and R.M. Fleming, *Phys. Rev. B* **48**, 9945 (1993).